Tau Positron Emission Tomographic Imaging in Aging and Early Alzheimer Disease

Keith A. Johnson, MD,[1,2,3,4,5] Aaron Schultz, PhD,[1,4,6] Rebecca A. Betensky, PhD,[7,8] J. Alex Becker, PhD,[1,3] Jorge Sepulcre, MD,[1,3,5,6] Dorene Rentz, PsyD,[2,4,5] Elizabeth Mormino, PhD,[2,4] Jasmeer Chhatwal, MD,[2,4,5] Rebecca Amariglio, PhD,[2,4,5] Kate Papp, PhD,[2,4,5] Gad Marshall, MD,[2,4,5] Mark Albers, MD,[2,5] Samantha Mauro, BS,[1,3] Lesley Pepin, BS,[1,3] Jonathan Alverio, BS,[1,3] Kelly Judge, BS,[1,3] Marlie Philiossaint, BS,[1,3] Timothy Shoup, PhD,[1,3] Daniel Yokell, PharmD,[1,3,5] Bradford Dickerson, MD,[1,2,5,6] Teresa Gomez-Isla, MD,[2,5] Bradley Hyman, MD,[2,5] Neil Vasdev, PhD,[1,3,5] and Reisa Sperling, MD[2,4,5,6]

Objective: Detection of focal brain tau deposition during life could greatly facilitate accurate diagnosis of Alzheimer disease (AD), staging and monitoring of disease progression, and development of disease-modifying therapies.
Methods: We acquired tau positron emission tomography (PET) using ^{18}F T807 (AV1451), and amyloid-β PET using ^{11}C Pittsburgh compound B (PiB) in older clinically normal individuals, and symptomatic patients with mild cognitive impairment or mild AD dementia.
Results: We found abnormally high cortical ^{18}F T807 binding in patients with mild cognitive impairment and AD dementia compared to clinically normal controls. Consistent with the neuropathology literature, the presence of elevated neocortical ^{18}F T807 binding particularly in the inferior temporal gyrus was associated with clinical impairment. The association of cognitive impairment was stronger with inferior temporal ^{18}F T807 than with mean cortical ^{11}C PIB. Regional ^{18}F T807 was correlated with mean cortical ^{11}C PiB among both impaired and control subjects.
Interpretation: These findings suggest that ^{18}F T807 PET could have value as a biomarker that reflects both the progression of AD tauopathy and the emergence of clinical impairment.

ANN NEUROL 2016;79:110–119

Alzheimer disease (AD) is neuropathologically defined and staged by the presence and distribution of 2 proteinaceous deposits, extracellular amyloid β (Aβ) and intracellular tau.[1,2] Until recently these lesions could not be detected during life, and their presence and distribution could only be evaluated at autopsy. A breakthrough reported in 2004 enabled researchers using positron emission tomography (PET) with ^{11}C Pittsburgh compound B (PiB) to detect Aβ deposits in living humans, and Aβ PET is now widely used in clinical trials of anti-Aβ therapies to identify individuals with AD pathology.[3] The detection of Aβ by PET tracers with very high molecular specificity has been confirmed by histopathologic correlation studies.[4,5] More recently, Kolb and

View this article online at wileyonlinelibrary.com. DOI: 10.1002/ana.24546

Received Jun 25, 2015, and in revised form Sep 28, 2015. Accepted for publication Oct 17, 2015.

Address correspondence to Dr Johnson, Division of Nuclear Medicine and Molecular Imaging, Massachusetts General Hospital, 55 Fruit Street, Boston, MA 02114. E-mail: kajohnson@pet.mgh.harvard.edu

From the [1]Division of Nuclear Medicine and Molecular Imaging, [2]Department of Neurology, and [3]Department of Radiology, Massachusetts General Hospital; [4]Center for Alzheimer Research and Treatment, Department of Neurology, Brigham and Women's Hospital; [5]Harvard Medical School; [6]Athinoula A. Martinos Center for Biomedical Imaging and [7]Department of Medicine (Biostatistics Center), Massachusetts General Hospital; and [8]Harvard School of Public Health, Boston, MA

colleagues tested a family of compounds based on binding to tau-laden postmortem AD brain slices.[6] Candidate ligands were compared with autoradiography to evaluate human frontal cortex sections from brains with a range of tau and Aβ pathology. ^{18}F T807 did not bind Aβ, and its affinity, metabolic stability, and low nonspecific binding in white matter or normal gray matter were very favorable.[6] In an initial report, 2 patients with AD and 1 with mild cognitive impairment (MCI) had elevated ^{18}F T807 binding compared to 3 normal controls.[7] These findings, along with reports of additional tau PET radiopharmaceutical developments, including THK523, THK5105, THK5117, PBB3, and ^{18}F T808 (reviewed in Villemagne et al[8], led us to test whether ^{18}F T807 binding would be elevated in neocortical areas in impaired subjects compared to normal controls, whether the binding would be related to cognitive status, and whether ^{18}F T807 would correlate with ^{11}C PiB measures of Aβ deposition.[7–11] We also tested the hypothesis that extensive T807 retention would occur only in the setting of substantial cortical amyloid deposition, that is, whether cortical ^{18}F T807 would be most common in subjects with elevated ^{11}C PiB measures of Aβ deposition in cortex.[7–11]

Subjects and Methods

Participants

Participants were recruited from the Harvard Aging Brain Study, a longitudinal study on aging and AD, from Memory Disorders Clinics at the Massachusetts General and Brigham and Women's Hospitals, and from the Massachusetts Alzheimer's Disease Research Center. All participants provided informed consent and were studied under protocols approved by the Partners Human Research Committee. All subjects underwent at least 1 comprehensive medical and neurological evaluation, and none had medical or neurological disorders that might contribute to cognitive dysfunction; a history of alcoholism, drug abuse, or head trauma; or a family history of autosomal dominant AD. None was clinically depressed at the time of study (Geriatric Depression Scale < 11) or had other psychiatric illnesses.[12] Each participant underwent a cognitive evaluation that included the Mini-Mental State Examination (MMSE), the Clinical Dementia Rating (CDR) Scale, and the Logical Memory delayed recall (LM).[13–15]

Participants were either clinically normal (CN) or cognitively impaired (Table 1). CN subjects (n = 56) had a CDR global score of 0, MMSE > 25, and performance within 1.5 standard deviation (SD) of age- and education-adjusted norms on cognitive testing at the time of recruitment into the Harvard Aging Brain Study.[15–18] Cognitively impaired participants fulfilled National Institute on Aging research criteria for either MCI (n = 13; global CDR = 0.5) or AD dementia (n = 6; global CDR = 1).[19,20] Patients with atypical clinical syndromes,

TABLE 1. Demographics

Characteristic	All	CN	MCI	AD	MCI/AD
No. (% F)	75 (43)	56 (48)	13 (23)	6 (33)	19 (26)
Age, yr	73 ± 8 [49–90]	75 ± 6 [65–89]	71 ± 9 [59–90]	63 ± 12 [49–78]	69 ± 10 [49–90][a]
Education, yr	16 ± 3 [12–20]	16 ± 3 [12–20]	17 ± 3 [12–20]	14 ± 3 [12–18]	16 ± 3 [12–20]
MMSE	28 ± 4 [11–30]	29 ± 1 [26–30]	26 ± 2 [22–30][a]	17 ± 5 [11–23][a]	24 ± 5 [11–30][a]
CDR-SB	1 ± 2 [0–11]	0 ± 0 [0–1.5]	2 ± 1.5 [0–5.5][a]	6 ± 4 [2.5–11][a]	3 ± 3 [0–11][a]
^{11}C PiB DVR	1.32 ± 0.3 [1.05–2]	1.24 ± 0.2 [1.05–1.81]	1.48 ± 0.3 [1.07–1.92][a]	1.76 ± 0.21 [1.45–2][a]	1.57 ± 0.3 [1.07–2][a]

Values are mean ± standard deviation [range] unless otherwise noted.
AD = Alzheimer disease dementia; CDR-SB = Clinical Dementia Rating, sum of boxes; CN = cognitively normal; DVR = distribution volume ratio; F = female; MCI = mild cognitive impairment; MMSE = Mini-Mental State Examination; PiB = Pittsburgh compound B.
[a]Differs from CN, $p < 0.05$.

such as posterior cortical atrophy, semantic dementia, or Dementia with Lewy bodies, were not included. Because of the symptomatic continuum between MCI and mild AD dementia, and the smaller numbers of participants in impaired groups compared to the CN group, the majority of analyses were performed with a combined MCI/AD impaired group.

Image Acquisition and Processing

For PET, ^{18}F T807 (AV1451) was prepared at Massachusetts General Hospital with a radiochemical yield of $14 \pm 3\%$ and specific activity of 216 ± 60GBq/μmol at the end of synthesis (60 minutes), and validated for human use.[21] ^{11}C PiB was prepared and PET data were acquired as described previously.[16] All PET data were acquired using a Siemens/CTI (Knoxville, TN) ECAT HR + scanner (3-dimensional mode, 63 image planes, 15.2cm axial field of view, 5.6mm transaxial resolution, and 2.4mm slice interval). ^{11}C PiB PET was acquired with a 8.5 to 15mCi bolus injection followed immediately by a 60-minute dynamic acquisition in 69 frames (12×15 seconds, 57×60 seconds). ^{18}F T807 was acquired from 80 to 100 minutes after a 9.0 to 11.0mCi bolus injection in 4×5-minute frames. PET data were reconstructed and attenuation corrected, and each frame was evaluated to verify adequate count statistics and absence of head motion. The mean $\pm$ SD lag time between ^{18}F T807 and MMSE and CDR ratings was 4.9 ± 3.5 months; between ^{18}F T807 and ^{11}C PiB PET imaging, it was 3.5 ± 2.6 months.

Magnetic resonance imaging (MRI) was performed on a 3T Tim Trio (Siemens) and included a magnetization-prepared rapid gradient-echo (MPRAGE) processed with FreeSurfer (FS) as described previously to identify gray–white and pial surfaces to permit region of interest (ROI) parcellation as follows: cerebellar gray, hippocampus, and the following Braak stage–related cortices: entorhinal (ER), parahippocampal (PH), inferior temporal (IT), fusiform (FF), and posterior cingulate (PC), as described previously.[16,22–25]

To evaluate the anatomy of cortical T807 binding, each individual PET data set was rigidly coregistered to the subject's MPRAGE data using SPM8 (Function Imaging Laboratory, Wellcome Department of Cognitive Neurology, London, UK). The cortical ribbon and subcortical ROIs defined by MRI as described above were transformed into the PET native space; PET data were sampled within each right–left ROI pair. standardized uptake value ratio (SUVR) values were represented graphically on vertices at the pial surface. PET data were not partial volume corrected.

^{18}F T807 specific binding was expressed in FS ROIs as the SUVR to cerebellum, similar to a previous report, using the FS cerebellar gray ROI as reference. For voxelwise analyses, each subject's MPRAGE was registered to the template MRI in SPM8, and the spatially transformed SUVR PET data were smoothed with an 8mm Gaussian kernel to account for individual anatomic differences.[7]

^{11}C PiB PET data were expressed as the distribution volume ratio (DVR) with cerebellar gray as reference tissue; regional time–activity curves were used to compute regional DVRs for each ROI using the Logan graphical method applied to data from 40 to 60 minutes after injection.[16,26] ^{11}C PiB retention was assessed using a large cortical ROI aggregate that included frontal, lateral temporal, and retrosplenial cortices (FLR) as described previously.[17,27]

Statistical Analyses

^{18}F T807 SUVR in CN and MCI/AD were compared both voxelwise and within FS-defined ROIs. PET ROI measures in each group were correlated with age using Spearman rho, with Bonferroni-adjusted alpha levels of 0.0083 (0.05/6 ROIs). The associations of APOEe4 carrier status with PET ROI were assessed with Wilcoxon tests. Effect sizes for clinical group classification in individual ROIs were evaluated with Mann–Whitney U tests and expressed as Cohen d. ^{11}C PIB FLR was used as a continuous measure of Aβ and also as a dichotomous measure, with high Aβ defined as FLR DVR > 1.2.[18] One MCI subject was classified as high Aβ on the basis of low cerebrospinal fluid (Aβ1–42 = 195pg/ml; ADmark; Athena Diagnostics, Marlborough, MA) and did not have PiB data available. Correlations between mean cortical PiB and inferior temporal ^{18}F T807 measures as well as relationships with age, MMSE, CDR sum of boxes (CDR-SB), and LM were evaluated with Spearman rho. MMSE and CDR-SB were also evaluated as ordinal data using cumulative logit models and estimating a separate log odds for each cutpoint of MMSE or CDR-SB.

Results

Demographic and Biomarker Measures

Table 1 gives the participant characteristics. The MCI/AD group in comparison to the CN group was younger ($p < 0.05$), was more impaired on the MMSE and CDR ($p < 0.05$), and had higher ^{11}C PiB DVR ($p < 0.05$).

In the MCI/AD group, greater age was associated with higher ^{18}F T807 binding in PH (rho = -0.61, $p < 0.006$), IT (rho = -0.70, $p < 0.001$), FF (rho = -0.59, $p < 0.008$), and PC (rho = -0.81, $p < 0.001$). In the CN group: (1) greater age was associated with higher PiB DVR (rho = 0.38, $p < 0.004$) and higher ^{18}F T807 SUVR binding in IT (rho = 0.46, $p < 0.001$); and (2) APOEe4 carrier status (median ages: 17 e4 carriers, 72 years; 39 noncarriers, 74 years) was associated with PiB DVR ($p < 0.009$), but not with ^{18}F T807 binding in any ROI at a 0.05 level of significance. Neither gender nor years of education was associated with any PET measure in either group.

^{18}F T807 Cortical Binding Correspondence with Expectations Based on Neuropathological Studies

Although direct image to tissue correspondence was not assessed in this in vivo study, the patterns of cortical ^{18}F T807 binding visualized with surface-projected SUVR thresholds were anatomically consistent with the ordinal Braak staging scheme (0, I/II, III/IV, and V/VI) as

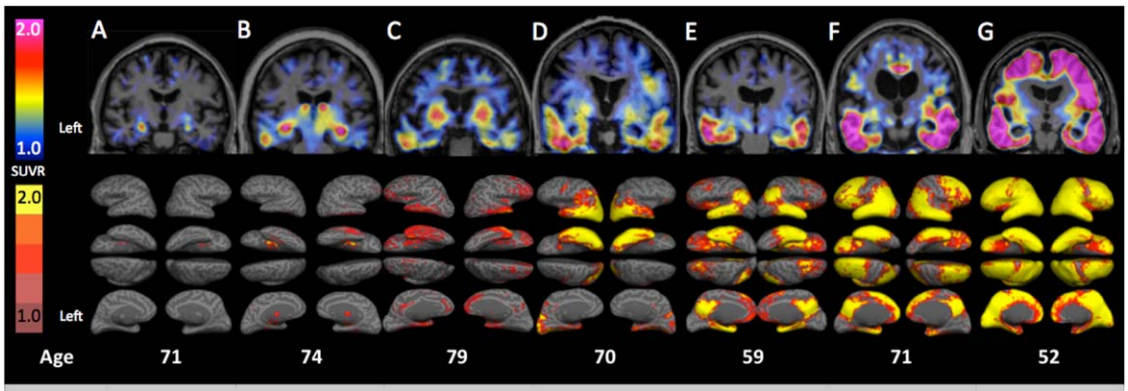

Age	71	74	79	70	59	71	52
MMSE	30	30	29	27	26	23	11
PiB (DVR)	Low (1.0)	High (1.2)	High (1.8)	High (1.5)	High (1.7)	High (1.5)	High (1.5)
Dx	CN	CN	CN	MCI	MCI	AD	AD
PET Braak	0, I-II	III-IV	III-IV	III-IV	III-IV	V-VI	V-VI

FIGURE 1: Cortical patterns of 18F T807 binding. Coronal ^{18}F T807 positron emission tomographic (PET) images (top row) and whole-brain surface renderings of standardized uptake value ratio (SUVR; cerebellar reference; second row) from 3 clinically normal (CN) and 4 impaired (2 mild cognitive impairment [MCI] and 2 mild Alzheimer dementia [AD] dementia) participants. Top: (A) A 71-year-old CN subject with low amyloid β (Aβ) by Pittsburgh compound B (PiB) PET (mean cortical distribution volume ratio [DVR] = 1.0) had low, nonspecific ^{18}F T807 binding in cortex, consistent with a Braak stage less than III/IV. (B) A 74-year-old CN subject with high Aβ (DVR = 1.2) with ^{18}F T807 binding in inferior temporal cortex, left > right, consistent with Braak stage III/IV. (C) A 79-year-old CN subject with high Aβ (DVR = 1.8) had binding in inferior temporal neocortex, consistent with Braak stage of III/IV. B and C show focally intense subcortical uptake that is likely due to off-target binding (see Discussion). (D–G) Cognitively impaired participants all with high Aβ and with successively greater levels of cortical ^{18}F T807 binding successively involving temporal, parietal, frontal, and occipital cortices. Bottom: ^{18}F T807 SUVR calculated at vertices (see Subjects and Methods) indicating the extent of cortical binding, with left hemisphere views (lateral, inferior, superior, medial) at left. The 52-year-old AD dementia patient (G) showed confluent ^{18}F T807 binding that is nearly pancortical, sparing only portions of primary cortex and consistent with Braak stage V/VI. Dx = classification; MMSE = Mini-Mental State Examination; PET Braak = estimate of Braak stages based on the anatomic pattern of T807 binding assessed visually and quantitatively in regions and full volume data.

follows.[22,28–30] Corresponding to Braak stages 0, I, or II, most CN subjects had low overall binding or only medial temporal lobe binding (Fig 1A–C), whereas more extensive neocortical binding in impaired subjects was always associated with much higher levels of temporal binding (see Fig 1D–G). The highest levels of neocortical binding, consistent with Braak stages V/VI, were associated with selective sparing of primary cortices (see Fig 1F–G). These anatomic patterns were confirmed quantitatively by the voxelwise and ROI measures described below, and their commonalities with Braak stages are summarized in the Discussion.

Regional ^{18}F T807 Binding in Cognitively Impaired Compared to CN Subject Groups

Contrast maps of voxelwise analyses revealed that group mean ^{18}F T807 cortical SUVR was elevated in the MCI/AD group in widespread neocortical regions, most prominently in inferior and lateral temporoparietal, parietooccipital, and posterior cingulate/precuneus (Fig 2). Significant but lower magnitude elevations were seen in frontal regions, whereas the least affected areas included the primary cortices, including calcarine, sensorimotor, and auditory. These data were consistent with the individual threshold-based anatomic assessments exemplified in Figure 1, in that statistical significance was either not reached or was lower in medial and inferior temporal cortex (see Fig 2) because many individuals in the CN group had modestly elevated SUVR in medial and inferior temporal regions, as confirmed with ROI analyses described below.

With ROI-based analyses (Fig 3), group comparison results fell into 3 categories:

1. Hippocampal ^{18}F T807 ROI binding was not significantly elevated in MCI/AD compared to CN, possibly due to off-target binding in adjacent structures (exemplified in Fig 1B); this potential confound is the topic of a separate investigation.[31]
2. In ER and PH, ^{18}F T807 binding was significantly higher in MCI/AD than in CN, but with notable

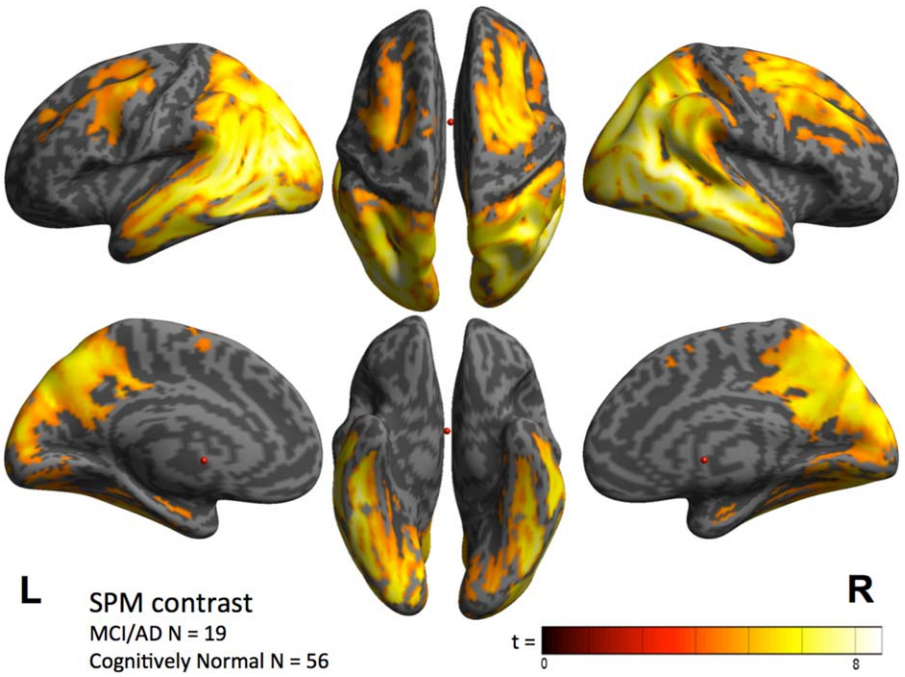

FIGURE 2: Cortical distribution of T807 binding: contrast between the combined mild cognitive impairment (MCI)/Alzheimer disease (AD) group (n = 19) and the cognitively normal group (n = 56; threshold $p < 10^{-5}$).

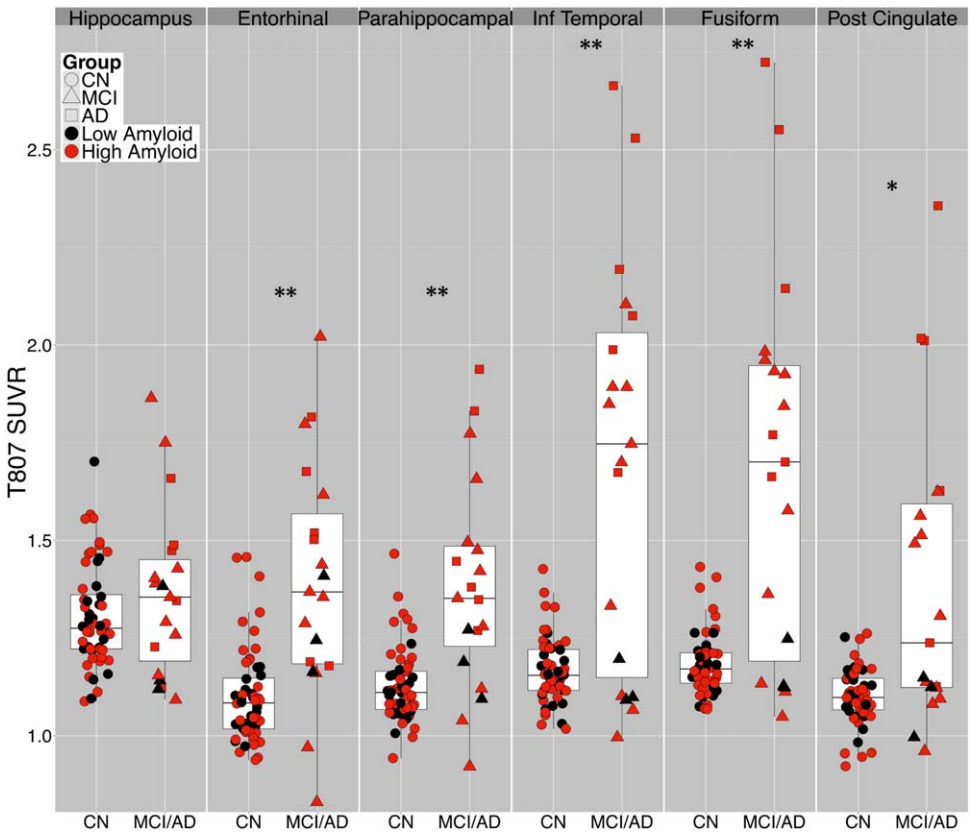

FIGURE 3: Regional T807 binding according to diagnostic group. T807 standardized uptake value ratio (SUVR) in regions of interest are shown by diagnostic group (clinically normal [CN], circles; mild cognitive impairment [MCI], triangles; Alzheimer disease [AD], squares) and amyloid status (high amyloid β [red] = Pittsburgh compound B distribution volume ratio $\geq$ 1.2), showing range, mean, and interquartile range; *t* test: *$p < 0.01$, **$p < 0.001$.

TABLE 2. T807 Binding in ROIs, Comparing MCI, AD, and Combined MCI/AD Groups with CN Subjects

ROI	CN, n = 56	MCI, n = 13	MCI, *d*	AD, n = 6	AD, *d*	MCI/AD	MCI/AD, *d*
PiB DVR	1.24 (0.18)	1.48 (0.30)	1.12[a]	1.76 (0.21)	2.72[b]	1.57 (0.30)	1.50[b]
Inferior temporal	1.17 (0.08)	1.47 (0.40)	1.60	2.19 (0.36)	7.63[b]	1.69 (0.51)	1.97[c]
Fusiform	1.18 (0.08)	1.49 (0.39)	1.70	2.09 (0.46)	5.87[b]	1.68 (0.49)	1.94[b]
Posterior cingulate	1.10 (0.07)	1.24 (0.23)	1.22[a]	1.73 (0.48)	3.98[b]	1.40 (0.39)	1.43[b]
Parahippocampal	1.13 (0.09)	1.31 (0.25)	1.37[a]	1.54 (0.28)	3.32[b]	1.38 (0.27)	1.61[b]
Entorhinal	1.10 (0.12)	1.36 (0.32)	1.47[c]	1.48 (0.26)	2.76[b]	1.40 (0.26)	1.62[b]
Hippocampus	1.31 (0.13)	1.36 (0.23)	0.32	1.39 (0.19)	0.58	1.37 (0.22)	0.38

d = Cohen *d*, effect size of group versus CN.
[a] $p < 0.05$,
[b] $p < 10^{-3}$,
[c] $p < 0.01$, as defined by Mann–Whitney *U* probability value of group versus CN. The Bonferroni-adjusted probability value threshold for 6 brain regions is 0.008. We did not correct for analyses of different subgroups of subjects within regions due to the high correlation among these subgroups and overconservatism of Bonferroni in that setting.
AD = Alzheimer disease dementia; CN = cognitively normal; DVR = distribution volume ratio; MCI = mild cognitive impairment; PiB = Pittsburgh compound B; ROI = region of interest.

overlap between groups and a right-skewed distribution of CN subjects.

3. In IT and FF, group mean differences were greater than in ER and PH and the overall distribution appears bimodal; all CN subjects had SUVR < 1.5 and all AD had SUVR > 1.5.

These differences were reflected in the effect sizes for AD versus CN, for example, Cohen $d = 7.63$ for IT (Table 2). In the MCI group, 7 of 13 had IT and FF SUVR < 1.5, that is, within the range of CN, whereas the remaining 6 had SUVR > 1.5, within the range of AD. Of the 7 MCI brains with IT T807 SUVR > 1.7, the same 7 individuals also had the highest binding in ER and FF, and 6 of the 7 had the highest binding in PH. MCI subjects with ^{18}F T807 SUVR > 1.5 in IT and FF were significantly (*U* tests) younger (63.8 ± 4.5 vs 77.4 ± 7.6 years; $p < 0.01$) and more impaired on MMSE (24.7 ± 2 vs 28.1 ± 2; $p < 0.01$) and on CDR-SB (1.1 ± 0.6 vs 3.0 ± 1.5; $p < 0.05$) than those with SUVR < 1.5. In addition, ^{11}C PiB DVR was elevated (>1.2) in all subjects with IT and FF ^{18}F T807 SUVR > 1.25.

^{18}F T807 and PiB Binding in Relation to Clinical Status and to Each Other

In the MCI/AD group, greater inferior temporal ^{18}F T807 SUVR was related to greater impairment on MMSE, CDR-SB, and LM (Fig 4); similar but weaker associations (lower rho values) were observed between greater PiB DVR and greater impairment on MMSE, CDR-SB, and LM. Inferior temporal ^{18}F T807 binding was associated with higher mean cortical PiB retention in both the full sample and in separate analyses of CN and MCI/AD (Fig 5). Across the full sample, inferior temporal ^{18}F T807 SUVR was > 1.3 only in those individuals with high PiB DVR.

Discussion

We evaluated ^{18}F T807, a PET radiopharmaceutical selective for tau pathology, by comparing clinically normal individuals to patients classified clinically as MCI or mild AD dementia. Large differences in ^{18}F T807 neocortical binding were detected between clinically defined groups; for example, Cohen *d* was 7.6 for AD dementia versus CN in inferior temporal lobe. Furthermore, ^{18}F T807 levels were correlated with measures of cognitive and functional impairment both across the entire sample and within the impaired group. This initial experience suggests that tau PET measures may be useful as a molecular imaging biomarker distinguishing impaired from unimpaired individuals, tracking progression of disease, and assessing response to putative disease-modifying treatments. ^{18}F T807 binding in the MCI/AD group was especially high in neocortical regions, including inferior temporal lobe, consistent with neuropathologic studies in which tau pathology at Braak stages III/IV or higher has been associated with AD dementia.[22,23,32]

Binding of the ^{18}F T807 ligand occurs specifically at sites of tauopathy, raising the possibility that when PET signal is sufficient to emerge from background, in vivo detection and anatomic staging of tau deposition is possible.[6] It has long been hypothesized on the basis of

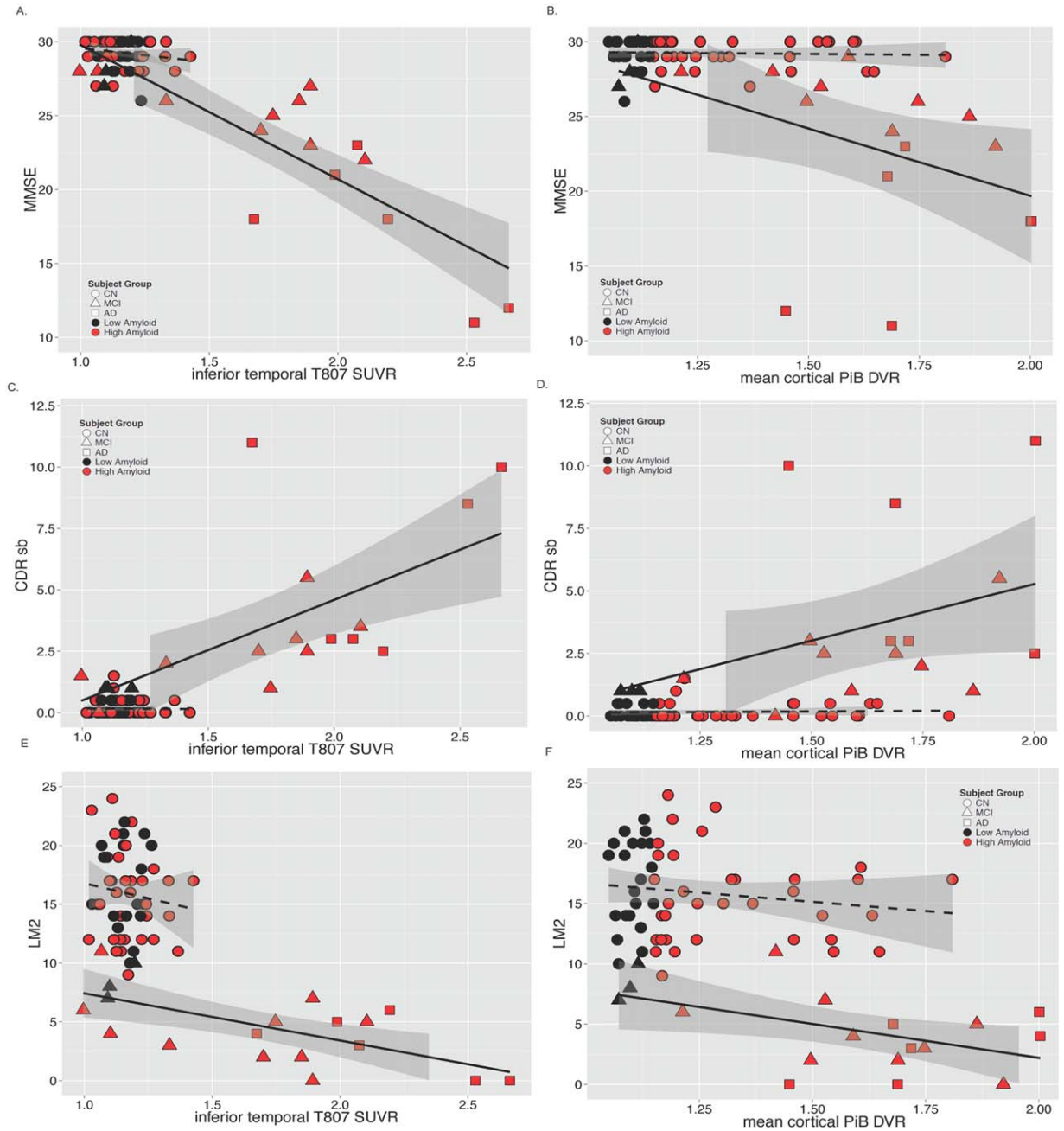

FIGURE 4: Correlations of tau pathology measured with ^{18}F T807 and amyloid β (Aβ) pathology measured with ^{11}C Pittsburgh compound B (PiB) with Mini-Mental State Examination (MMSE), Clinical Dementia Rating sum of boxes (CDR sb), and Logical Memory 2 (LM2). Clinically normal (CN) subjects are represented with circles, mild cognitive impairment (MCI) with triangles, and Alzheimer disease (AD) with squares; red indicates high Aβ (PiB distribution volume ratio [DVR] > 1.2), and black represents low Aβ (PiB DVR ≤ 1.2). Spearman correlations (rho) follow for each positron emission tomography measure versus MMSE, CDR sb, or LM2. (A) MMSE versus inferior temporal T807 standardized uptake value ratio (SUVR): CN, n = 56, Spearman $\rho = -0.20$, $p = 0.14$; cumulative logit, log odds ratio (OR) = 4.20, $p = 0.18$. MCI/AD, n = 19, Spearman $\rho = -0.83$, $p < 10^{-4}$; cumulative logit, log OR = 6.89, $p < 10^{-4}$. All, n = 75, Spearman $\rho = -0.46$, $p < 10^{-4}$; cumulative logit, log OR = 7.28, $p < 10^{-4}$. (B) MMSE versus mean cortical PiB DVR: CN, n = 56, Spearman $\rho = -0.05$, $p = 0.72$; cumulative logit, log OR = 0.75, $p = 0.59$. MCI/AD, n = 18, Spearman $\rho = -0.63$, $p = 0.005$; cumulative logit, log OR = 5.38, $p = 0.003$. All, n = 74, Spearman $\rho = -0.40$, $p < 10^{-3}$; cumulative logit, log OR = 4.59, $p < 10^{-4}$. (C) CDR sb versus inferior temporal T807 SUVR: CN, n = 56, Spearman $\rho = 0.02$, $p = 0.89$; cumulative logit, log OR = −0.72, $p = 0.84$. MCI/AD, n = 19, Spearman $\rho = 0.75$, $p = 0.0002$; cumulative logit, log OR = −4.93, $p = 0.0002$. All, n = 75, Spearman $\rho = 0.42$, $p = 0.0002$; cumulative logit, log OR = −6.05, $p < 10^{-4}$. (D) CDR sb versus mean cortical PiB DVR: CN, n = 56, Spearman $\rho = 0.04$, $p = 0.77$; cumulative logit, log OR = −0.97, $p = 0.54$. MCI/AD, n = 18, Spearman $\rho = 0.52$, $p = 0.03$; cumulative logit, log OR = −3.85, $p = 0.02$. All, n = 74, Spearman $\rho = 0.39$, $p = 0.0005$; cumulative logit, log OR = −4.33, $p < 10^{-4}$. (E) LM2 versus inferior temporal T807 SUVR: CN, n = 56, Spearman $\rho = -0.10$, $p = 0.45$. MCI/AD, n = 19, Spearman $\rho = -0.58$, $p = 0.01$. All, n = 75, Spearman $\rho = -0.39$, $p = 0.0006$. (F) LM2 versus mean cortical PiB DVR: CN, n = 56, Spearman $\rho = -0.12$, $p = 0.36$. MCI/AD, n = 18, Spearman $\rho = -0.50$, $p = 0.04$. All, n = 74, Spearman $\rho = -0.42$, $p = 0.0002$.

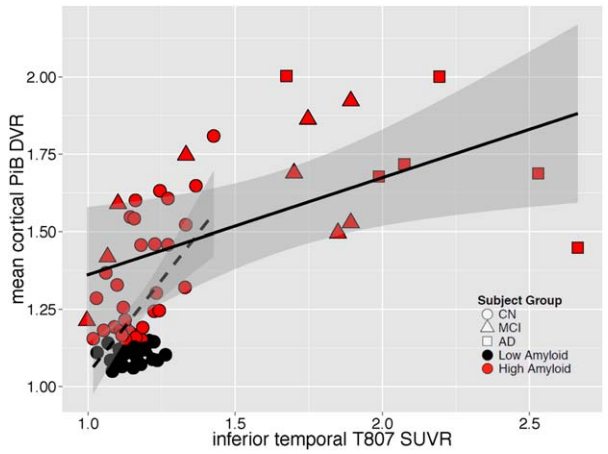

FIGURE 5: Correlations of tau pathology measured with inferior temporal ^{18}F T807 and amyloid β (Aβ) pathology measured with mean cortical ^{11}C Pittsburgh compound B (PiB). Clinically normal (CN) subjects are represented with circles, mild cognitive impairment (MCI) with triangles, and Alzheimer disease (AD) with squares; red indicates high Aβ (PiB distribution volume ratio [DVR] > 1.2), and black indicates low Aβ (PiB DVR ≤ 1.2). Separate linear fit lines (dashed for CN, solid for MCI/AD) are shown to aid inspection. SUVR = standardized uptake value ratio. CN, n = 56, Spearman $\rho = 0.32$, $p = 0.02$. MCI/AD, n = 18, Spearman $\rho = 0.51$, $p = 0.03$. All, n = 74, Spearman $\rho = 0.53$, $p < 10^{-4}$.

autopsy material that tau deposition spreads beyond the entorhinal cortex in temporal proximity to cognitive impairment.[2,22–24,32] Our data support this hypothesis because we found that greatly elevated ^{18}F T807 binding in temporal neocortex (eg, SUVR > 1.5) was only observed in subjects with cognitive impairment. If these observations are verified in longitudinal samples where the time course can be examined, the development of tau pathological lesions in the temporal neocortex will be a risk factor detectable by PET for increased likelihood of emergence of the dementing phase of AD. This may well enable more accurate clinical diagnosis and be a useful outcome measure in clinical trials.

Across the full sample of subjects, several features of the pattern of ^{18}F T807 binding were qualitatively consistent with expected anatomic patterns, whereas other features were not consistent. For example, as expected, successively higher binding was seen in inferolateral temporal regions, and temporoparietal to frontal regions.[22] The somewhat stronger statistical signal seen in occipitoparietal compared to frontal neocortical regions (see Fig 2) is consistent with neuropathologic observations.[22,23] In addition, widespread binding consistent with later Braak stages spared primary cortices and was invariably accompanied by high levels of binding in the temporal lobe.

Two features were not consistent with expectations based on pathoanatomical studies. Contrary to Braak staging predictions, we did not see a consistent pattern of successively greater ^{18}F T807 in the hippocampus with more advanced disease. We postulate that this observation may be due in part to off-target binding adjacent to hippocampus; however, PET detection of 18F T807 binding in hippocampus is particularly susceptible to artifact when atrophy is a factor, due to small volume and surrounding cerebrospinal fluid.

Second, ^{18}F T807 binding to an area near the substantia nigra is more likely to be off-target because limited neurofibrillary pathology occurs in this structure. The potential for off-target binding of ^{18}F T807 or other ligands may be a limitation for their use in staging tau pathology. Ex vivo autoradiography may clarify this issue by identifying off-target ^{18}F T807 binding, including sources of a suspected confound of signal spill-in from structures adjacent to the hippocampus (see Fig 1).[31] Postmortem correlative studies are clearly necessary, as they continue to be for Aβ PET, to identify biological substrates. However, preliminary experience with ^{18}F T807 suggests that a PET-based staging of AD pathology could be established on the basis of cortical ^{18}F T807 binding for tau, which could be useful either alone or in combination with measures of Aβ. Technical factors will require continued evaluation for potential clinical implementation of ^{18}F T807 PET, including choice of window for imaging based on kinetic modeling, choice of reference region, and image quantitation protocols.[7]

We observed a significant relationship between age and inferior temporal ^{18}F T807 binding within the relatively restricted age range of our normal participants, consistent with large autopsy studies.[2] Studies of ^{18}F T807 PET in younger subjects will be required to test whether entorhinal cortex binding in older normal subjects exceeds that in younger subjects, as predicted by reports with Braak staging, and whether this binding represents a tauopathy that, although primarily age-related, is accompanied by subtle but measurable levels of cognitive impairment.[33,34] It must be born in mind, however, that compared to the microscopy-based Braak staging scheme, tau PET staging of AD is inherently limited because of the lower resolution and sensitivity of PET. For example, current PET technology is not likely to detect or distinguish tau deposition in entorhinal cortex that separates Braak 0 from 1 or 2.

Conversely, the subset of clinically normal older individuals with elevations in both temporal lobe ^{18}F T807 binding and in mean cortical Aβ estimated with PiB or other Aβ ligands may be at elevated risk for imminent clinical and cognitive decline. We observed a trend-level association in CN subjects between elevated

^{18}F T807 and worse MMSE, and further evaluation using more sensitive cognitive measures is warranted.

In the combined CN and MCI/AD sample, levels of neocortical tau deposition of SUVR > 1.3 were only observed in individuals with elevated Aβ (PiB DVR > 1.2). This finding is consistent with the idea that along the AD trajectory high levels of tau in neocortex are only seen in those with high Aβ burden; however, more extensive evaluation in larger samples will be required to determine whether this is a robust finding. Although longitudinal studies with serial ^{18}F T807 imaging will be critical to understand the time course of tau spread, and to determine whether the pattern of anatomic spread is similar to the pattern of tau deposition described in autopsy studies, our findings thus far suggest that ^{18}F T807 PET imaging may prove valuable in monitoring progression of AD-related neurodegeneration.

Acknowledgment

This study was supported by the NIH National Institute on Aging (R01 AG046396 to K.A.J., P01 AG036694 to R.A.S. and K.A.J., P50 AG00513421 to K.A.J. and R.A.S.), Fidelity Biosciences, Harvard Neurodiscovery Center, and Alzheimer's Association.

Author Contributions

K.A.J. contributed to conceptualization of the study, analysis and interpretation of data, drafting and revision of the report, and statistical analysis. R.A.B. contributed to drafting and revision of the report and to the statistical analysis. A.S., J.A.B., J.S., D.R., E.M., J.C., R.A., K.P., G.M., M.A., B.D., T.G.-I., B.H., N.V., and R.S. contributed to analysis and interpretation of data, and drafting and revision of the report. S.M., L.P., J.A., K.J., M.P., T.S., and D.Y. contributed to drafting and revision of the report, and provided technical support.

Potential Conflicts of Interest

K.A.J.: personal fees, Piramal, Novartis, Siemens, Lilly/Avid, Janssen, AZTherapies, Roche, Genentech, GE Healthcare, Biogen Idec, ISIS Pharma; grants, Lilly/Avid, Merck, Janssen, Eisai, Biogen Idec, NIH, Michael J. Fox Foundation. E.M.: funding, NIH. M.A.: grants, Merck, Takeda; nonfinancial support, Merck; consultancy, Takeda, Merck. T.S.: patent, "Radiosynthesis of Tau Radio-Pharmaceuticals" (2014) WO 2014194169 A1 20141204. B.D.: consultancy, Merck, Forum. B.H.: personal fees, Siemens, Calico, ISIS Pharma, Eli Lilly, Neurophage, Pfizer, Biogen, Genentech, Sanofi, AbbVie, Novartis; grants, Siemens, Biogen Idec, BMS, AZTherapies, Acumen, Prothena, Fidelity Biosciences, Spark, Intellect; family member employed, Novartis. N.V.: patent, "Radiosynthesis of Tau Radio-Pharmaceuticals" (2014) WO 2014194169 A1 20141204. R.S.: consultancy, Roche, Biogen Idec, Genentech, Bracket; grants, Janssen, Eli Lilly, NIH.

References

1. Hyman BT, Phelps CH, Beach TG, et al. National Institute on Aging-Alzheimer's Association guidelines for the neuropathologic assessment of Alzheimer's disease. Alzheimers Dement 2012;8:1–13.
2. Nelson PT, Alafuzoff I, Bigio EH, et al. Correlation of Alzheimer disease neuropathologic changes with cognitive status: a review of the literature. J Neuropathol Exp Neurol 2012;71:362–381.
3. Klunk WE, Engler H, Nordberg A, et al. Imaging brain amyloid in Alzheimer's disease with Pittsburgh compound-B. Ann Neurol 2004;55:306–319.
4. Clark CM, Pontecorvo MJ, Beach TG, et al. Cerebral PET with florbetapir compared with neuropathology at autopsy for detection of neuritic amyloid-β plaques: a prospective cohort study. Lancet Neurol 2012;11:669–678.
5. Rinne JO, Wong DF, Wolk DA, et al. [(18)F]Flutemetamol PET imaging and cortical biopsy histopathology for fibrillar amyloid β detection in living subjects with normal pressure hydrocephalus: pooled analysis of four studies. Acta Neuropathol 2012;124:833–845.
6. Xia C-F, Arteaga J, Chen G, et al. [(18)F]T807, a novel tau positron emission tomography imaging agent for Alzheimer's disease. Alzheimers Dement 2013;9:666–676.
7. Chien DT, Bahri S, Szardenings AK, et al. Early clinical PET imaging results with the novel PHF-tau radioligand [F-18]-T807. J Alzheimers Dis 2013;34:457–468.
8. Villemagne VL, Fodero-Tavoletti MT, Masters CL, Rowe CC. Tau imaging: early progress and future directions. Lancet Neurol 2015;14:114–124.
9. Okamura N, Furumoto S, Fodero-Tavoletti MT, et al. Non-invasive assessment of Alzheimer's disease neurofibrillary pathology using 18F-THK5105 PET. Brain 2014;137:1762–1771.
10. Harada R, Okamura N, Furumoto S, et al. Comparison of the binding characteristics of [18F]THK-523 and other amyloid imaging tracers to Alzheimer's disease pathology. Eur J Nucl Med Mol Imaging 2013;40:125–132.
11. Villemagne VL, Furumoto S, Fodero-Tavoletti MT, et al. In vivo evaluation of a novel tau imaging tracer for Alzheimer's disease. Eur J Nucl Med Mol Imaging 2014;41:816–826.
12. Yesavage JA, Brink TL, Rose TL, et al. Development and validation of a geriatric depression screening scale: a preliminary report. J Psychiatr Res 1983;17:37–49.
13. Wechsler D. WMS-R: Wechsler Memory Scale–revised. San Antonio, TX: Psychological Corp, 1987.
14. Folstein MF, Folstein SE, McHugh PR. "Mini-Mental State." A practical method for grading the cognitive state of patients for the clinician. J Psychiatr Res 1975;12:189–198.
15. Morris JC. The Clinical Dementia Rating (CDR): current version and scoring rules. Neurology 1993;43:2412–2414.
16. Becker JA, Hedden T, Carmasin J, et al. Amyloid-β associated cortical thinning in clinically normal elderly. Ann Neurol 2011;69:1032–1042.
17. Amariglio RE, Becker JA, Carmasin J, et al. Subjective cognitive complaints and amyloid burden in cognitively normal older individuals. Neuropsychologia 2012;50:2880–2886.

18. Mormino EC, Betensky RA, Hedden T, et al. Amyloid and APOE e4 interact to influence short-term decline in preclinical Alzheimer disease. Neurology 2014;82:1760–1767.

19. Albert MS, Dekosky ST, Dickson D, et al. The diagnosis of mild cognitive impairment due to Alzheimer's disease: recommendations from the National Institute on Aging-Alzheimer's Association workgroups on diagnostic guidelines for Alzheimer's disease. Alzheimers Dement 2011;7:270–279.

20. McKhann GM, Knopman DS, Chertkow H, et al. The diagnosis of dementia due to Alzheimer's disease: recommendations from the National Institute on Aging-Alzheimer's Association workgroups on diagnostic guidelines for Alzheimer's disease. Alzheimers Dement 2011;7:263–269.

21. Shoup TM, Yokell DL, Rice PA, et al. A concise radiosynthesis of the tau radiopharmaceutical, [(18) F]T807. J Labelled Comp Radiopharm, 2013;56:736–740.

22. Braak H, Alafuzoff I, Arzberger T, et al. Staging of Alzheimer disease-associated neurofibrillary pathology using paraffin sections and immunocytochemistry. Acta Neuropathol 2006;112:389–404.

23. Braak H, Braak E. Frequency of stages of Alzheimer-related lesions in different age categories. Neurobiol Aging 1997;18:351–357.

24. Delacourte A, Sergeant N, Wattez A, et al. Tau aggregation in the hippocampal formation: an ageing or a pathological process? Exp Gerontol 2002;37:1291–1296.

25. Fischl B, Salat DH, van der Kouwe AJ, et al. Sequence-independent segmentation of magnetic resonance images. Neuroimage 2004;23(suppl 1):S69–S84.

26. Logan J. Graphical analysis of reversible radioligand binding from time-activity measurements. J Cereb Blood Flow Metab 1990;10: 740–747.

27. Hedden T, Van Dijk KRA, Becker JA, et al. Disruption of functional connectivity in clinically normal older adults harboring amyloid burden. J Neurosci 2009;29:12686–12694.

28. Arriagada PV, Marzloff K, Hyman BT. Distribution of Alzheimer-type pathologic changes in nondemented elderly individuals matches the pattern in Alzheimer's disease. Neurology 1992;42: 1681–1688.

29. Arriagada PV, Growdon JH, Hedley-Whyte ET, Hyman BT. Neurofibrillary tangles but not senile plaques parallel duration and severity of Alzheimer's disease. Neurology 1992;42(3 pt 1):631–639.

30. Gómez-Isla T, Price JL, McKeel DW Jr, et al. Profound loss of layer II entorhinal cortex neurons occurs in very mild Alzheimer's disease. J Neurosci 1996;16:4491–4500.

31. Marquie M, Normandin M, Vanderburg C, et al. Towards the validation of novel PET tracer T807 on postmortem human brain tissue samples. Paper presented at: 9th Human Amyloid Imaging Conference; January 14–16, 2015; Miami, FL.

32. Serrano-Pozo A, Qian J, Monsell SE, et al. Examination of the clinicopathologic continuum of Alzheimer disease in the autopsy cohort of the National Alzheimer Coordinating Center. J Neuropathol Exp Neurol 2013;72:1182–1192.

33. Nelson PT, Abner EL, Schmitt FA, et al. Brains with medial temporal lobe neurofibrillary tangles but no neuritic amyloid plaques are a diagnostic dilemma but may have pathogenetic aspects distinct from Alzheimer disease. J Neuropathol Exp Neurol 2009;68:774–784.

34. Crary JF, Trojanowski JQ, Schneider JA, et al. Primary age-related taupathy (PART): a common pathology associated with human aging. Acta Neuropathol 2014;128:755–766.